

Copula Based Fusion of Clinical and Genomic Machine Learning Risk Scores for Breast Cancer Risk Stratification

Agnideep Aich^{1*}, Sameera Hewage² and Md Monzur Murshed³

¹ Department of Mathematics, University of Louisiana at Lafayette, Lafayette, LA, USA.

² Department of Physical Sciences & Mathematics, West Liberty University, West Liberty, WV, USA

³ Department of Mathematics and Statistics, Minnesota State University, Mankato, MN, USA

Abstract

Clinical and genomic models are both used to predict breast cancer outcomes, but they are often combined using simple linear rules that do not account for how their risk scores relate, especially at the extremes. Using the METABRIC breast cancer cohort, we studied whether directly modeling the joint relationship between clinical and genomic machine learning risk scores could improve risk stratification for 5-year cancer-specific mortality. We created a binary 5-year cancer-death outcome and defined two sets of predictors: a clinical set (demographic, tumor, and treatment variables) and a genomic set (gene-expression z -scores). We trained several supervised classifiers, such as Random Forest and XGBoost, and used 5-fold cross-validated predicted probabilities as unbiased risk scores. These scores were converted to pseudo-observations on $(0, 1)^2$ to fit Gaussian, Clayton, and Gumbel copulas. Clinical models showed good discrimination (AUC 0.783), while genomic models had moderate performance (AUC 0.681). The joint distribution was best captured by a Gaussian copula (bootstrap $p = 0.997$), which suggests a symmetric, moderately strong positive relationship. When we grouped patients based on this relationship, Kaplan-Meier curves showed clear differences: patients who were high-risk in both clinical and genomic scores had much poorer survival than those high-risk in only one set. These results show that copula-based fusion works in real-world cohorts and that considering dependencies between scores can better identify patient subgroups with the worst prognosis.

Introduction

Breast cancer is still a major cause of cancer deaths among women worldwide, with over two million new cases each year [Bray et al., 2018]. Data show that outcomes vary widely: five-year survival rates are high for localized cases but drop sharply for advanced or metastatic disease. Because of these differences, accurate risk assessment is needed to tailor treatments and focus intensive care on patients who are most likely to benefit.

Researchers now know that breast cancer is not a single disease but includes several biologically distinct subtypes. Gene-expression studies and subtype classifiers have identified groups,

*Corresponding author: Agnideep Aich, agnideep.aich1@louisiana.edu, ORCID: [0000-0003-4432-1140](https://orcid.org/0000-0003-4432-1140)

such as luminal A, luminal B, HER2-enriched, basal-like, and normal-like, each with unique molecular features and clinical outcomes [Parker et al., 2009]. Large projects, such as Molecular Taxonomy of Breast Cancer International Consortium (METABRIC), have collected detailed clinical and genomic data from thousands of patients, providing a clearer picture of breast tumor biology [Curtis et al., 2012, Pereira et al., 2016]. Still, even within the same subtype, there is considerable variation in patient outcomes, highlighting the need to combine different types of information.

Traditionally, breast cancer prognosis has been based on clinicopathologic factors like tumor size, grade, lymph-node status, hormone-receptor status, and HER2 expression. These markers are affordable, easy to collect, and straightforward to interpret, forming the basis of tools like the Nottingham Prognostic Index. However, clinical models alone may overlook important biological differences. Tumors that look alike under the microscope can behave very differently at the molecular level and respond differently to treatment.

Multigene tests like Oncotype DX, MammaPrint, and PAM50 have made gene-expression-based risk prediction a regular part of clinical care [Paik et al., 2004, van 't Veer et al., 2002, Parker et al., 2009]. These tests give information about tumor growth, hormone signaling, and subtypes that clinical markers alone cannot provide. However, studies show that gene-expression predictors do not always outperform clinical models, and their extra value can be limited at the population level [Neapolitan and Jiang, 2015, Liu et al., 2014]. For example, in the METABRIC study, combining clinical and gene-expression data improved survival predictions; however, clinical factors still provided a wealth of useful information [Neapolitan and Jiang, 2015, Liu et al., 2014]. This suggests that clinical and genomic predictors capture both shared and unique aspects of risk.

Modern machine learning (ML) methods have introduced new approaches to modeling risk in complex cancer genomics data. Flexible models, such as tree-based ensembles, can identify nonlinear effects, interactions, and complex relationships between genes and clinical factors. However, ML models can be influenced by specific features of the data and analysis choices, and reproducibility and generalizability remain significant concerns in oncology. In many studies using datasets like METABRIC, clinical and genomic features are either combined into one large dataset or their risk scores are simply added together [Neapolitan and Jiang, 2015, Liu et al., 2014]. These approaches assume that the risk factors are either independent or simply add up in a straightforward manner.

In reality, the impact of genomic information on prognosis can depend on a patient's clinical details, and vice versa. For instance, a gene-expression signature indicating high proliferation might have different implications for a young patient with node-positive disease compared to an older patient with small, node-negative tumors. To capture these context-specific effects, we need tools that can describe both the individual and joint behavior of clinical and genomic risk scores. Standard methods, such as linear combination or simply merging features, cannot easily reveal complex dependencies or cases where risk is high only when both clinical and genomic factors are extreme.

Copula models provide a structured approach to separating individual distributions from their dependence, making them a suitable fit for this problem [Nelsen, 2006]. A copula is a multivariate distribution with uniform marginals on $[0, 1]$ that connects single-variable models into a joint one [Sklar, 1959]. By choosing different copula types, we can model symmetric, lower-tail, upper-tail, or more complex relationships without limiting the form of the individual risk scores. In biomedical statistics, copulas have been used for bivariate survival data and multivariate event processes [Shih and Louis, 1995, Satten, 1996], and more recently for modeling

the spread of breast cancer [Gasparini and Humphreys, 2022]. Pair-copula and vine copula methods have also enhanced risk profiling before surgery, enabling the better identification of low-risk patients compared to standard methods [Sahin and Joe, 2024]. Outside medicine, copula-based fusion has been used to combine different scores in speaker verification and other pattern-recognition tasks, where modeling the dependence between outputs improves results over simple linear methods [Susyanto et al., 2015]. Copula concepts have also been included in Bayesian networks for genomic data and in hybrid ML frameworks for survival analysis [Zhang and Shi, 2017, Kim, 2025].

Even with this expanding research, we are not aware of any published studies that directly model the joint distribution of machine learning-derived clinical and genomic risk scores using copulas for breast cancer risk stratification. Most current methods treat the clinical and genomic components as either separate models, whose results are averaged, or as features in a single combined model. These approaches do not focus on the dependence between the risk scores and are not designed to detect extreme-risk interactions or mismatched risk patterns.

In this study, we test whether combining clinical and genomic ML risk scores using copulas can improve five-year cancer-specific mortality prediction in the METABRIC cohort [Curtis et al., 2012, Pereira et al., 2016]. We first built supervised ML models separately for clinical variables and high-dimensional mRNA expression, getting out-of-fold risk predictions for each patient. These predictions are then converted to values on the unit interval and used to fit Gaussian, Clayton, and Gumbel copulas, which represent different types of dependence. We assess the model’s fit using a bootstrap-calibrated Cramér–von Mises test and utilize the best copula to define joint risk groups. Finally, we compare survival differences across groups defined by clinical-only, genomic-only, and copula-fused risk scores.

The primary aims of this study are:

1. To develop clinical and genomic machine learning risk scores for predicting five-year cancer-specific mortality in the METABRIC cohort.
2. To model the joint dependence structure of these risk scores using parametric copulas from multiple families.
3. To evaluate whether copula-based fusion improves patient stratification compared with using clinical or genomic scores independently.
4. To identify clinically meaningful subgroups characterized by concordant or discordant clinical–genomic risk and to assess their survival outcomes.

Our results demonstrate that copula-based modeling effectively captures the relationships between clinical and genomic ML risk scores, creating combined risk groups with improved survival separation compared to using either model alone. More generally, this approach demonstrates that copulas can be a valuable tool for combining various machine-learning predictors in biomedical risk modeling and personalized cancer care.

The next section reviews related work on clinical and genomic prognostic modelling and the application of copulas in biomedical statistics.

Related Work

In this section, we review prior work on clinical and genomic prognostic modelling, multimodal machine learning, and copula-based methods, and we position our copula-based fusion of clinical and genomic risk scores within this landscape.

Clinical and Genomic Prognostic Models in Breast Cancer

Traditionally, breast cancer prognosis has relied on clinical and pathological factors like tumor size, nodal status, grade, and hormone receptor status. Tools such as the Nottingham Prognostic Index, Adjuvant! Online and PREDICT are still widely used because they utilize affordable, routinely collected data and provide clear risk estimates at the bedside [Galea et al., 1992, Ravdin et al., 2001, Wishart et al., 2010]. However, tumors with similar clinical profiles can have very different outcomes, showing the biological diversity of breast cancer and the limitations of using only clinical models.

High-throughput genomic profiling has led to more molecularly informed methods for assessing risk. Tests like Oncotype DX, MammaPrint, and PAM50 utilize gene-expression patterns to generate recurrence scores that aid in guiding chemotherapy decisions for early-stage breast cancer [Paik et al., 2004, van 't Veer et al., 2002, Parker et al., 2009]. These tests reveal tumor biology that standard pathology cannot see and are now part of international guidelines. Still, studies show that these genomic tests often get much of their predictive power from genes related to cell growth and may only slightly improve risk prediction when added to strong clinical models. Because of this, researchers are now combining clinical and genomic information, seeing them as complementary sources of risk.

The METABRIC cohort is one of the most studied datasets that matches clinical and genomic data in breast cancer. Neapolitan and Jiang utilized METABRIC to demonstrate that combining 21 clinical variables with genome-wide expression data enhances survival prediction compared to using clinical data alone. They also found that random survival forests work better than Cox models in this diverse setting [Neapolitan and Jiang, 2015]. Liu and colleagues looked at differences across molecular subtypes and found that clinical variables often provided more useful information than gene-expression profiles, even within these subgroups [Liu et al., 2014]. These findings support the idea that clinical and genomic features capture different but overlapping risks, suggesting the use of two-view modeling instead of combining all features into a single feature set.

Multimodal Machine Learning and Current Fusion Strategies

Researchers have used machine learning (ML) methods on clinical, genomic, and multi-omics data to find complex patterns and interactions. Techniques such as random forests, gradient boosting, penalized regression, and deep neural networks have been employed to develop prognostic scores from gene-expression and multi-omics data, often outperforming traditional regression models in research settings. However, ML models that use only genomic data can be affected by batch effects, changes in patient groups, and platform-specific issues, which can make them less reliable in new settings.

Many studies now focus on combining clinical and genomic information in unified ML frameworks. Most often, this is achieved by merging clinical and molecular features into a single large input or by combining separate risk scores with fixed or learned weights. For example, Neapolitan and Jiang's METABRIC analysis combined clinical and gene-expression features in a single random survival forest model [Neapolitan and Jiang, 2015]. Other methods employ stacking or ensemble learning to combine predictors, yet still treat the overall risk as predominantly additive. While these models often outperform single-view models, they do not directly model how clinical and genomic risks interact with each other. This means they may miss important nonlinear or extreme-risk patterns needed to identify patients at very high or mismatched risk.

Copulas in Biomedical Statistics and Model Fusion

Copula models provide a structured approach to describing the relationship between multiple variables, separating their individual behavior from their dependence on each other [Nelsen, 2006]. In biostatistics, copulas have been utilized to analyze bivariate and multivariate survival outcomes, enabling flexible modeling even when data are censored. Shih and Louis developed methods for estimating association in copula models for bivariate survival data, showing that these approaches can handle complex relationships in time-to-event outcomes [Shih and Louis, 1995]. More recently, Gasparini and Humphreys employed a copula-based model to link tumor growth, nodal spread, and distant metastasis in breast cancer, while maintaining the individual models' interpretability [Gasparini and Humphreys, 2022].

Copulas have also been used to model genomic and biomedical data outside of survival analysis. Zhang and Shi developed a mixture copula Bayesian network for multimodal genomic data, enabling flexible, non-Gaussian relationships in network models and enhancing predictions compared to Gaussian Bayesian networks [Zhang and Shi, 2017]. In perioperative risk modeling and other clinical uses, pair-copula (vine) models have been used for patient risk profiling, and studies show that copula-based classifiers can provide better calibration and lower Brier scores than traditional regression or random-forest models when risk factors have uneven dependence in the tails [Sahin and Joe, 2024].

Copula-based fusion has also been applied outside of medicine to combine machine learning models. For example, Cumani developed a score-level fusion model for speaker verification, where a Gaussian copula models the joint distribution of scores from different systems, leading to better calibration and verification than linear fusion [Susyanto et al., 2015]. In survival analysis, Kim combined copula-based random forests with deep learning to estimate varied treatment effects, showing that copulas can capture complex dependencies that standard ensemble methods might miss [Kim, 2025]. These studies show that copulas can be a useful tool for combining models and making predictions that account for dependencies.

Positioning of the Present Study

Despite this growing research, the use of copulas to combine machine-learning risk scores from separate clinical and genomic sources remains largely unexplored in oncology. Most breast cancer prognosis studies either combine clinical and genomic variables into a single feature set or use linear or additive methods to predict risk, assuming simple relationships. Previous copula work in biomedicine has focused on modeling survival outcomes, metastasis, or multiple biomarkers [Shih and Louis, 1995, Gasparini and Humphreys, 2022, Zhang and Shi, 2017], not on merging ML risk scores.

This study addresses a gap by using parametric copulas (Gaussian, Clayton, and Gumbel) to analyze the empirical ranks of out-of-fold clinical and genomic machine learning risk scores in the METABRIC cohort. By modeling different types of dependence such as symmetric, lower-tail, and upper-tail, we show how clinical and genomic risks change together across the risk spectrum, especially in high-risk areas. This copula-based method forms joint risk groups that differ from those created by simply combining risk scores, and it helps identify subgroups with either similar high clinical and genomic risks or distinct risk profiles. To our knowledge, this is the first application of copula-based fusion to combine multimodal machine learning risk scores for breast cancer prognosis, providing a general approach to integrate different predictors in biomedical risk modeling.

In the next section, we outline the background and methods behind our copula-based ap-

proach to combining clinical and genomic machine learning risk scores.

Preliminaries

In this section, we summarize the main probabilistic and statistical tools used in our analysis. These include copulas and tail dependence, the specific copula families we considered (Gaussian, Clayton, and Gumbel), the Cramér–von Mises goodness-of-fit test with parametric bootstrap, the machine learning models used to build risk scores, and the survival analysis framework for evaluation.

Copulas and Pseudo-observations

A bivariate copula $C : [0, 1]^2 \rightarrow [0, 1]$ is a joint distribution function with uniform marginals that captures the dependence structure between two random variables independently of their marginal scales [Sklar, 1959, Nelsen, 2006, Joe, 1997]. By Sklar’s theorem [Sklar, 1959], any bivariate cumulative distribution function (cdf) H with continuous marginals F_X and F_Y can be uniquely decomposed as

$$H(x, y) = C(F_X(x), F_Y(y)), \quad (1)$$

where C is the copula of (X, Y) .

In this work, X and Y are the clinical and genomic machine learning risk scores, respectively. To work on the copula scale, we convert these scores into *pseudo-observations* by ranking:

$$U_i = \frac{\text{rank}(X_i)}{n+1}, \quad V_i = \frac{\text{rank}(Y_i)}{n+1}, \quad i = 1, \dots, n, \quad (2)$$

where n is the number of patients and $\text{rank}(\cdot)$ is the average rank. The pairs (U_i, V_i) lie in $(0, 1)^2$ and are approximately sampled from the underlying copula. Any subsequent quantity computed from C (for example, tail-dependence coefficients) therefore depends only on the joint behaviour of the risk scores and not on their marginal calibration.

Tail Dependence

Tail dependence measures the strength of association in the extremes of a bivariate distribution. For a copula (U, V) with continuous marginals, the *upper* and *lower* tail-dependence coefficients are defined as [Nelsen, 2006, Joe, 1997]

$$\lambda_U = \lim_{q \rightarrow 1^-} \Pr(V > q \mid U > q), \quad (3)$$

$$\lambda_L = \lim_{q \rightarrow 0^+} \Pr(V \leq q \mid U \leq q), \quad (4)$$

whenever the limits exist. Values of λ_U or λ_L close to 1 indicate strong clustering of extreme events, whereas values near 0 indicate tail independence.

In our setting, (U, V) represent the ranks of clinical and genomic risk scores. A positive upper-tail coefficient λ_U indicates that patients who are extreme high-risk clinically also tend to be extreme high-risk genetically, while a positive lower-tail coefficient λ_L would indicate co-occurrence of very low predicted risks. These coefficients provide an interpretable summary of how the two modalities interact in the most clinically relevant regions of the risk spectrum.

Gaussian, Clayton and Gumbel Copulas

We focus on three parametric copula families that capture different dependence patterns: a symmetric elliptical copula (Gaussian) and two Archimedean copulas (Clayton and Gumbel) [Nelsen, 2006, Joe, 1997].

Gaussian copula. Let Φ denote the standard normal cdf and Φ_ρ the bivariate normal cdf with correlation $\rho \in (-1, 1)$. The Gaussian copula is

$$C_\rho^{\text{Gauss}}(u, v) = \Phi_\rho(\Phi^{-1}(u), \Phi^{-1}(v)), \quad (u, v) \in (0, 1)^2. \quad (5)$$

We estimate ρ from Kendall's rank correlation τ via the usual relationship

$$\rho = \sin\left(\frac{\pi}{2}\tau\right), \quad (6)$$

which follows from the elliptical structure [Nelsen, 2006]. For $|\rho| < 1$, the Gaussian copula is tail-independent, with $\lambda_L = \lambda_U = 0$ [Nelsen, 2006].

Clayton copula. The Clayton copula [Clayton, 1978] is an Archimedean copula with parameter $\theta > 0$ and cdf

$$C_\theta^{\text{Clay}}(u, v) = (u^{-\theta} + v^{-\theta} - 1)^{-1/\theta}, \quad (u, v) \in (0, 1)^2. \quad (7)$$

Clayton exhibits lower-tail but not upper-tail dependence:

$$\lambda_L(\theta) = 2^{-1/\theta}, \quad \lambda_U(\theta) = 0. \quad (8)$$

Its Kendall's tau satisfies

$$\tau(\theta) = \frac{\theta}{\theta + 2}, \quad \iff \quad \theta = \frac{2\tau}{1 - \tau}, \quad (9)$$

which we use to obtain a method-of-moments estimate of θ from the empirical $\hat{\tau}(U, V)$.

Gumbel copula. The Gumbel (Gumbel-Hougaard) copula [Gumbel, 1960, Hougaard, 1986] is an Archimedean copula with parameter $\theta \geq 1$ and cdf

$$C_\theta^{\text{Gum}}(u, v) = \exp\left\{-\left[(-\log u)^\theta + (-\log v)^\theta\right]^{1/\theta}\right\}, \quad (u, v) \in (0, 1)^2. \quad (10)$$

Gumbel has positive upper-tail dependence but no lower-tail dependence [Nelsen, 2006]:

$$\lambda_U(\theta) = 2 - 2^{1/\theta}, \quad \lambda_L(\theta) = 0. \quad (11)$$

Kendall's tau is

$$\tau(\theta) = 1 - \frac{1}{\theta}, \quad \iff \quad \theta = \frac{1}{1 - \tau}, \quad \tau \in (0, 1). \quad (12)$$

Thus θ can again be estimated from the empirical $\hat{\tau}(U, V)$, and λ_U then follows in closed form.

Together, these three families allow us to compare a symmetric, tail-independent dependence model (Gaussian) with two asymmetric, tail-dependent models that emphasize either joint low-risk (Clayton) or joint high-risk (Gumbel) behaviour.

Cramér–von Mises Goodness-of-fit for Copulas

To assess how well a parametric copula family fits the empirical dependence between clinical and genomic risk scores, we use a Cramér–von Mises (CvM) statistic based on the empirical copula [Genest and Rivest, 1993, Genest et al., 2008, 2007]. Let

$$C_n(u, v) = \frac{1}{n} \sum_{i=1}^n \mathbf{1}\{U_i \leq u, V_i \leq v\} \quad (13)$$

denote the empirical copula of $(U_i, V_i)_{i=1}^n$, and let $C_{\hat{\theta}}$ be a fitted parametric copula with parameter(s) $\hat{\theta}$. The CvM discrepancy is

$$S_n = \frac{1}{n} \sum_{i=1}^n [C_n(U_i, V_i) - C_{\hat{\theta}}(U_i, V_i)]^2. \quad (14)$$

Because the null distribution of S_n depends on the chosen family and on $\hat{\theta}$, we approximate its sampling distribution by a parametric bootstrap [Genest et al., 2008, 2007]. Specifically, we repeatedly simulate pseudo-observations $(U_i^{(b)}, V_i^{(b)})_{i=1}^n$ from $C_{\hat{\theta}}$, recompute $S_n^{(b)}$ for each bootstrap sample, and estimate the p -value as

$$\hat{p} = \frac{1 + \sum_{b=1}^B \mathbf{1}\{S_n^{(b)} \geq S_n\}}{B + 1}, \quad (15)$$

with $B = 1000$ replications in our experiments. Higher p -values indicate better agreement between the parametric copula and the empirical dependence structure.

Machine Learning Risk Scores

We construct separate machine-learning risk scores from the clinical and genomic views using standard classifiers on tabular data. Let $Z^{(\text{clin})}$ denote the matrix of clinical predictors and $Z^{(\text{gen})}$ the matrix of genomic predictors, and let Y be the binary indicator of 5-year cancer-specific mortality.

For each view, we consider the following supervised learning models:

- **Logistic regression with elastic-net penalty (LR).** A generalized linear model that maps features to log-odds of the outcome, with combined ℓ_1 and ℓ_2 penalties to encourage sparsity and stabilize estimates [Cox, 1958, Zou and Hastie, 2005].
- **Random forest (RF).** An ensemble of decision trees trained on bootstrap samples with feature subsampling at each split, which captures nonlinearities and interactions while reducing variance through averaging [Breiman, 2001].
- **Gradient boosting (GB).** An additive ensemble of shallow trees fitted sequentially, where each new tree is trained to reduce the residual error of the current ensemble [Friedman, 2001].
- **Extreme gradient boosting (XGB).** A regularized implementation of gradient boosting with system-level optimizations and additional shrinkage/penalty terms for improved performance on tabular data [Chen and Guestrin, 2016], used when the `xgboost` library is available.

For each model and each view, we perform 5-fold stratified cross-validation and use out-of-fold predicted probabilities $\hat{p}_i^{(\text{clin})}$ and $\hat{p}_i^{(\text{gen})}$ as clinical and genomic risk scores, respectively. This cross-validation scheme avoids optimistic bias by ensuring that each patient’s risk score is obtained from a model that did not use that patient’s outcome for training. The final risk scores used for copula fitting correspond to the best-performing model in each view, as selected by cross-validated ROC-AUC.

Survival Analysis and ROC-AUC

Although the primary endpoint for model training is 5-year cancer-specific mortality, the METABRIC cohort also includes detailed follow-up times and censoring indicators. To visualize and compare long-term survival patterns across fused risk strata, we use the Kaplan-Meier estimator [[Kaplan and Meier, 1958](#)]. For a given subgroup, let $t_1 < t_2 < \dots < t_J$ be the distinct event times, and let d_j and r_j denote the numbers of events and patients at risk at time t_j . The Kaplan–Meier estimate of the survival function is

$$\hat{S}(t) = \prod_{t_j \leq t} \left(1 - \frac{d_j}{r_j}\right), \quad (16)$$

which provides a non-parametric estimate of the probability of remaining event-free beyond time t while accommodating right-censoring. We apply this estimator within joint clinical–genomic risk groups (e.g., low–low, high–clinical-only, high–genomic-only, high–high) defined from the fused copula model.

For discrimination performance, we use the area under the receiver operating characteristic curve (ROC-AUC) as the primary metric. Given model scores s_i and binary outcomes Y_i , ROC-AUC is the probability that a randomly chosen event case receives a higher score than a randomly chosen non-event case,

$$\text{AUC} = \Pr(s^+ > s^-) + \frac{1}{2} \Pr(s^+ = s^-), \quad (17)$$

and summarizes threshold-free ranking performance. ROC-AUC is computed separately for clinical-only, genomic-only, and copula-fused risk scores.

In the next section, we describe the METABRIC dataset.

Dataset Description

In this study, we used breast cancer data from the Molecular Taxonomy of Breast Cancer International Consortium (METABRIC), a large Canada–UK project that profiled primary breast tumors with clinical, pathological, and genomic measurements [[Curtis et al., 2012](#), [Pereira et al., 2016](#)]. The METABRIC cohort includes nearly 2,000 patients with long-term follow-up and is widely used as a benchmark for studying breast cancer subtypes and prognosis.

For our analyses, we used the processed file `METABRIC_RNA_Mutation.csv` from Kaggle, rather than reconstructing the data ourselves. This file, derived from METABRIC data on cBioPortal, combines curated clinical attributes, mRNA expression z scores for selected genes, mutation data, and survival outcomes for each patient. Using this processed file ensures transparency and allows other researchers with Kaggle access to reproduce our work.

Clinical Variables

The clinical part of the file has one row per patient and includes baseline and tumor-related variables. These cover demographic details, such as age at diagnosis, surgical information (including type of surgery, cancer type, detailed histological subtype), and measures of tumor cellularity and grade. The file also lists hormone receptor and HER2 status from laboratory tests, as well as molecular subtype labels such as PAM50 and three gene classifier categories. Other variables include treatment indicators (chemotherapy, hormone therapy, and radiotherapy), inferred menopausal status, cluster assignments, tumor laterality, lymph node counts, mutation count, Nottingham Prognostic Index, tumor size, and stage. Some variables have missing entries due to incomplete original records.

Survival information includes overall survival time in months and status indicators. The file provides

`overall_survival_months`, which records follow-up time from diagnosis, along with an overall survival status and a specific indicator for death from breast cancer. These variables are used to define the 5-year cancer death endpoint in our prediction models.

Genomic Variables

The genomic part of the file contains high-dimensional molecular data. For each patient, it includes mRNA expression z scores for several hundred genes. These scores indicate the degree to which each gene's expression in a tumor deviates from the mean in a reference group, expressed in standard deviations. Positive values mean upregulation, and negative values mean downregulation. The file also has binary indicators for gene mutations, showing whether a gene has a relevant somatic mutation in that tumor.

Taken together, the expression and mutation variables form a wide genomic feature matrix for each patient, while the clinical variables provide a complementary view of disease presentation and treatment. This structure naturally supports two-view analyses in which clinical and genomic predictors are modelled both separately and jointly.

Working Dataset for Analysis

For all analyses in this paper, we use `METABRIC_RNA_Mutation.csv` as our starting dataset. We first create a binary endpoint for 5-year cancer death from the survival variables, then focus on patients with enough follow-up to determine this outcome. In this filtered group, we define clinical and genomic predictor views and utilize them to train machine learning models that generate cross-validated risk scores for 5-year cancer-related mortality. The next section explains this methodology in detail, including endpoint definition, predictor view construction, the machine learning pipeline, and copula-based modeling of joint risk.

Methodology

Overview and Guiding Question

In this section, we describe the development, testing, and combination of clinical and genomic machine learning (ML) risk scores for patients in the METABRIC breast cancer cohort. Our primary question is straightforward: for the same group of patients, how do risk scores derived from routine clinical data and high-dimensional genomic data compare when predicting 5-year

cancer mortality, and what does their combined behavior reveal about patients at particularly high risk?

We approached the problem as a two-view prediction task. First, we created a binary outcome to show whether each patient died from cancer within 60 months of diagnosis, and included only patients with enough follow-up to assess this. Next, we divided the predictors into two groups. The clinical view encompasses standard clinical and pathological variables, including age at diagnosis, tumor size, nodal status, receptor status, treatment indicators, and other baseline characteristics. The genomic view includes mRNA expression and mutation features from the same patients.

For each view, we trained several supervised machine learning models to predict 5-year cancer death. We used 5-fold stratified cross-validation to get out-of-fold predicted probabilities for every patient in the dataset. These out-of-fold probabilities make up our clinical risk score and genomic risk score. They show how well each view alone predicts 5-year cancer death, without including the held-out patient in model training.

To examine the relationship between the two risk scores, we first converted them to pseudo-uniform variables using their empirical ranks and applied standard bivariate copula models, including the Gaussian, Clayton, and Gumbel copulas. We used these fitted copulas to calculate summary measures of overall and tail dependence, and assessed goodness-of-fit with the Cramér–von Mises statistic and a parametric bootstrap. Finally, we grouped individuals by their risk scores (for example, low in both, high in one, or high in both) and compared their survival outcomes using Kaplan–Meier curves.

The next section explains how we built the 5-year cancer-death endpoint using the METABRIC survival variables. It also shows how this process defines the analytic cohort for all later analyses.

Endpoint definition and analytic cohort

All analyses used the processed METABRIC dataset from Kaggle. For each patient, this file provides overall survival time in months, an overall survival status, and a specific indicator for death from breast cancer. In the code, these variables are called `overall_survival_months`, `overall_survival`, and `death_from_cancer`.

We created a binary endpoint for 5-year cancer death, using a fixed time window of 60 months. For each patient, we first recorded the survival time as

$$T = \text{overall_survival_months}.$$

Next, we defined an event indicator using the available status variables. If the `death_from_cancer` column was present, we used it as the main source for event status. If not, we used `overall_survival`. The code can handle both numeric encodings (0/1) and string labels such as “Died of Disease”, “Dead”, or “Living”. These values were converted to a binary status variable.

$$\Delta = \begin{cases} 1, & \text{if the record indicates death from cancer,} \\ 0, & \text{if the record indicates that the patient is alive or not known} \\ & \text{to have died from cancer.} \end{cases}$$

Any records with unrecognized status labels were marked as missing at this point.

The 5-year endpoint Y was then defined as

$$Y = \begin{cases} 1, & \text{if } \Delta = 1 \text{ and } T \leq 60 \text{ months,} \\ 0, & \text{if } \Delta = 1 \text{ and } T > 60 \text{ months,} \\ 0, & \text{if } \Delta = 0 \text{ and } T \geq 60 \text{ months,} \\ \text{missing,} & \text{otherwise.} \end{cases}$$

In summary, a patient is counted as a 5-year cancer-death event if they died from cancer within 60 months. Patients who are alive or who die after 60 months are considered non-events. If a patient is censored or lost to follow-up before 60 months without a recorded cancer death, we assign a missing value for Y and exclude them from further analyses. This approach avoids making assumptions about patients without enough follow-up to determine their 5-year status.

After calculating Y , we kept only patients with a non-missing 5-year endpoint and reset the row indices. This filtered dataset and the binary outcome vector Y define the analytic cohort used for all predictive modeling and dependence analyses in the rest of the paper.

In the next section, we explain how we split the variables in this cohort into clinical and genomic groups and prepared them for supervised machine learning.

Clinical and Genomic Predictor Views

We used all predictor variables from the filtered analytic cohort described earlier. In our code, we first separated variables with a clinical role from those that represent genomic information.

We defined the clinical view by starting with the clinical and pathological variables listed in the Kaggle description of the METABRIC file. These included patient identifier, age at diagnosis, type of breast surgery, cancer type and detailed histology, measures of tumour cellularity and grade, oestrogen, progesterone, and HER2 receptor status (from immunohistochemistry and molecular assays), PAM50 and related molecular subtype labels, treatment indicators (chemotherapy, hormone therapy, radiotherapy), inferred menopausal status, integrative cluster assignment, tumour laterality, lymph-node involvement, mutation count, Nottingham prognostic index, OncoTree diagnostic code, tumour size, and tumour stage. We then removed all survival-related variables (`overall_survival_months`, `overall_survival`, `death_from_cancer`) to ensure the clinical predictors did not include any direct information about the outcome or follow-up time. The remaining columns comprised the clinical predictor matrix used for downstream modeling.

We defined the genomic view as everything left after removing the clinical variables, patient identifier, and survival variables from the analytic cohort. These remaining columns were treated as genomic features, mainly mRNA expression z -scores for a panel of genes, mutation indicators, and other high-dimensional molecular data. Since there are many more genomic features than patients, we used a simple unsupervised filtering step to select a manageable subset. We focused on numeric genomic columns, calculated the variance of each feature across patients, and kept the 50 features with the highest variance. This filtering step does not utilize the outcome and helps remove features that are nearly constant and unlikely to contribute to classification. The final set of high-variance genomic features formed the predictor matrix for the genomic view.

In the next section, we explain how we preprocessed these clinical and genomic predictors and used them to train supervised machine learning models that generate cross-validated risk scores for 5-year cancer death.

Supervised Machine Learning for Clinical and Genomic Risk Scores

We trained supervised classification models using the clinical and genomic predictor views to predict the binary 5-year cancer-death outcome. Our aim was not to find one best algorithm, but to generate well-calibrated, cross-validated risk scores from each view for later joint analysis with copula models.

We used the same modeling pipeline for each view. We defined X_{clin} as the clinical predictor matrix, X_{gen} as the genomic predictor matrix, and Y as the binary 5-year cancer-death outcome. In each view, we separated predictors into numeric and categorical variables based on their data type. We imputed numeric variables with the median value and categorical variables with the most common category. Numeric variables were standardized to have a mean of zero and a variance of one, and categorical variables were one-hot encoded. These preprocessing steps were included in the model pipeline, so during cross-validation, imputation, scaling, and encoding were fitted only on the training data and then applied to the test fold.

After preprocessing, we tested several common classification algorithms: penalized logistic regression with elastic-net penalty, random forest, gradient boosting, and XGBoost when available. For each view, we trained and evaluated each model using 5-fold stratified cross-validation. In each fold, the model was trained on four-fifths of the data and used to predict class probabilities for the remaining fifth. Cycling through the folds gave a complete set of out-of-fold predicted probabilities for all patients. We compared these predictions to the true binary outcome using the area under the receiver operating characteristic curve (ROC-AUC) as the performance metric.

For each view, we chose the model with the highest cross-validated ROC-AUC as the main risk-score generator. The out-of-fold predicted probabilities from this model were kept as the view-specific machine learning risk scores. We use \hat{p}_{clin} for the predicted probability of 5-year cancer death from the best clinical model, and \hat{p}_{gen} for the best genomic model. Each value in these vectors comes from a model that did not use that patient in training, which helps reduce optimistic bias and makes the risk scores suitable for later dependence modeling.

We also recorded the cross-validated ROC-AUC for each candidate model in each view. These summary values serve as a benchmark for assessing how well the clinical and genomic views independently predict 5-year cancer death rates. In the next subsection, we explain how we used \hat{p}_{clin} and \hat{p}_{gen} to create pseudo-observations on the unit square and fit parametric copula models to capture the joint dependence between the two risk scores.

Copula Modelling of Joint Risk Scores

After obtaining cross-validated risk scores from the clinical and genomic data, we modeled their joint behavior using bivariate copulas. Let

$$\hat{p}_{\text{clin}} = (\hat{p}_{\text{clin},1}, \dots, \hat{p}_{\text{clin},n}), \quad \hat{p}_{\text{gen}} = (\hat{p}_{\text{gen},1}, \dots, \hat{p}_{\text{gen},n})$$

represent the clinical and genomic risk scores for the n patients in the study. Since copulas require variables with uniform margins, we first converted each risk score to pseudo-observations on the unit interval by ranking:

$$U_i = \frac{\text{rank}(\hat{p}_{\text{clin},i})}{n+1}, \quad V_i = \frac{\text{rank}(\hat{p}_{\text{gen},i})}{n+1}, \quad i = 1, \dots, n,$$

where $\text{rank}(\cdot)$ means the average rank if there are ties. The pairs (U_i, V_i) fall within $(0, 1)^2$ and make up the empirical sample for fitting the copula.

We considered three standard parametric copula families that capture different patterns of dependence: the Gaussian copula, the Clayton copula, and the Gumbel copula. In all cases, we used Kendall's τ as the basis for parameter estimation. First, we computed the sample Kendall's tau between (U_i, V_i) :

$$\hat{\tau} = \tau(U, V).$$

For the Gaussian copula, the dependence parameter is the correlation coefficient ρ , which we found using the standard relationship

$$\hat{\rho} = \sin\left(\frac{\pi}{2}\hat{\tau}\right).$$

For the Clayton copula, which shows lower-tail dependence, we calculated the parameter θ_{Clay} using

$$\hat{\theta}_{\text{Clay}} = \frac{2\hat{\tau}}{1 - \hat{\tau}}.$$

We set a small positive lower bound in the code if $\hat{\tau}$ was not positive. For the Gumbel copula, which shows upper-tail dependence, we got the parameter θ_{Gum} from

$$\hat{\theta}_{\text{Gum}} = \frac{1}{1 - \hat{\tau}}.$$

We explicitly applied the constraint $\hat{\theta}_{\text{Gum}} \geq 1$. These formulas are the standard links between Kendall's τ and the copula parameters for these families, and they avoid the need for iterative optimization.

For each fitted copula, we calculated tail-dependence coefficients using known closed-form formulas. The Gaussian copula has zero asymptotic tail dependence if $|\rho| < 1$. The Clayton copula has non-zero lower-tail dependence and zero upper-tail dependence, while the Gumbel copula has non-zero upper-tail dependence and zero lower-tail dependence. The code calculates these coefficients from the estimated parameters and saves them for reporting purposes.

To check how well each copula family fits the data, we used a Cramér–von Mises goodness-of-fit statistic based on the empirical copula. The empirical copula at each observed pair (U_i, V_i) is defined as

$$C_n(U_i, V_i) = \frac{1}{n} \sum_{j=1}^n \mathbf{1}\{U_j \leq U_i, V_j \leq V_i\}.$$

Given a fitted copula $C(u, v; \theta)$ with parameter θ , we calculated the model-based values $C(U_i, V_i; \hat{\theta})$ at the same points and then computed the Cramér–von Mises statistic

$$S = \frac{1}{n} \sum_{i=1}^n (C_n(U_i, V_i) - C(U_i, V_i; \hat{\theta}))^2.$$

We calibrated this statistic using a parametric bootstrap. For each copula family, we generated B bootstrap samples of size 1000 from the fitted copula with parameter $\hat{\theta}$. We used direct simulation for the Gaussian copula and Algorithm I of Genest and Rivest, 1993 [[Genest and Rivest, 1993](#)] for the Clayton and Gumbel copulas. For each bootstrap sample, we recalculated the Cramér–von Mises statistic to create a reference distribution $\{S^{(b)} : b = 1, \dots, B\}$. We then estimated the bootstrap p -value for the fitted copula as

$$\hat{p} = \frac{1 + \sum_{b=1}^B \mathbf{1}\{S^{(b)} \geq S\}}{B + 1}.$$

We summarized the goodness-of-fit for each copula family by reporting the observed statistic S and its bootstrap p -value. The copula with the largest p -value was chosen as the best-fitting model for the joint distribution of (U, V) .

To visually compare the empirical and fitted dependence structures, the code creates contour plots of the fitted copula overlaid on the pseudo-observations. It also makes heatmaps that compare the empirical copula with the copula evaluated on a regular grid over $(0, 1)^2$. These plots are later used in the Results section to show the quality of fit and the pattern of joint dependence between the clinical and genomic risk scores.

In the next section, we explain how we used the estimated risk scores to define joint risk strata and how we connected these strata to the observed survival outcomes in the METABRIC cohort.

Joint Risk Strata and Survival Analysis

To connect the joint behavior of clinical and genomic risk scores to actual outcomes, we created simple joint risk groups and examined their survival over time. We used the original survival data from the METABRIC file. For each patient, we recorded the follow-up time in months, noted as $T = \text{overall_survival_months}$, and used an event indicator based on `death_from_cancer` when available, or `overall_survival` otherwise. We normalized these labels to a binary status variable, as done when building the endpoint. In this analysis, we used the full follow-up time and event indicator, without applying the 60-month cut-off. This means the survival curves show the entire observed follow-up for each risk group.

Next, we used the cross-validated clinical and genomic risk scores, \hat{p}_{clin} and \hat{p}_{gen} , to divide patients into four separate groups based on whether their scores were above or below the median. Here, m_{clin} and m_{gen} are the sample medians for the clinical and genomic risk scores. Each patient was placed into one of these groups:

- **low-low**: patients with $\hat{p}_{\text{clin}} \leq m_{\text{clin}}$ and $\hat{p}_{\text{gen}} \leq m_{\text{gen}}$;
- **high-clinical-only**: patients with $\hat{p}_{\text{clin}} > m_{\text{clin}}$ and $\hat{p}_{\text{gen}} \leq m_{\text{gen}}$;
- **high-genomic-only**: patients with $\hat{p}_{\text{clin}} \leq m_{\text{clin}}$ and $\hat{p}_{\text{gen}} > m_{\text{gen}}$;
- **high-both**: patients with $\hat{p}_{\text{clin}} > m_{\text{clin}}$ and $\hat{p}_{\text{gen}} > m_{\text{gen}}$.

These four groups are: patients with a low estimated risk from both models, patients marked as high risk only by the clinical model, patients marked as high risk only by the genomic model, and patients marked as high risk by both models simultaneously.

For each group, we estimated the Kaplan-Meier survival curve using the full follow-up time T and the event indicator. We left out groups with very small sample sizes from the plot to avoid unstable curves. The Kaplan-Meier curves facilitate easy comparison of survival across the four joint risk groups. The high-both group is a practical way to identify patients at high risk, since both clinical and genomic models agree that these patients are at elevated risk. If our method is effective, this group should have the lowest survival rate.

This finishes the methods section. We defined a 5-year cancer-death endpoint, built clinical and genomic predictors, trained cross-validated machine learning models to obtain risk scores for each view, modeled the relationship between these scores using copulas, and linked the joint risk groups to observed survival. In the next section, we present the results obtained by applying this approach to the METABRIC cohort.

Results

This section presents the main findings from our analysis of the METABRIC cohort. We begin by summarizing the accuracy of the clinical and genomic machine learning risk scores in predicting outcomes and their distribution. Next, we describe how the two scores are related using copula models, and finally, we examine the long-term survival outcomes of patients with high risk in both scores.

Predictive Performance of Clinical and Genomic Models

Here, we summarize the accuracy of clinical and genomic machine learning models in predicting 5-year cancer death in the METABRIC cohort and describe the distribution of risk scores. We then shift from examining each score separately to analyzing how the two scores interact using copula models.

Table 1 shows the cross-validated ROC-AUC for each classifier and data type. For the clinical data, all four models performed similarly, with ROC-AUCs ranging from approximately 0.76 to 0.78. The random forest was the best clinical model (AUC 0.783), followed by elastic-net logistic regression (AUC 0.762), gradient boosting (AUC 0.760), and XGBoost (AUC 0.763). For the genomic data, performance was lower but still better than chance. The random forest again performed best (AUC 0.681), while the other genomic models had AUCs ranging from 0.647 to 0.657. These results show that clinical predictors alone are better at distinguishing 5-year cancer death than the gene-expression panel, but the genomic data still provide useful prognostic information.

Table 1: Cross-validated ROC-AUC for 5-year cancer-death prediction by model and view.

Model	View	ROC-AUC
Elastic-net logistic regression	Clinical	0.762
Random forest	Clinical	0.783
Gradient boosting	Clinical	0.760
XGBoost	Clinical	0.763
Elastic-net logistic regression	Genomic	0.657
Random forest	Genomic	0.681
Gradient boosting	Genomic	0.655
XGBoost	Genomic	0.647

Figure 1 displays the ROC curves for the random forest models using clinical and genomic data. The clinical risk score curve is always above the genomic curve, showing its higher AUC. Both curves are clearly separated from the 45-degree reference line, which means they have real predictive value. The clinical curve rises more sharply at low false-positive rates, suggesting that clinical variables alone can rank patients by 5-year risk fairly well, while genomic data add a smaller extra signal.

Figure 2 shows the distributions of the cross-validated risk scores. Clinical risk scores span a wide range, from nearly 0 to approximately 0.8, with fewer patients at higher risk levels. Genomic risk scores are more tightly grouped, with values mostly falling between 0.15 and 0.55, and a few outliers at either end. This difference aligns with the higher AUC for the clinical model, as clinical scores more effectively separate low- and high-risk patients, while genomic scores are more compressed.

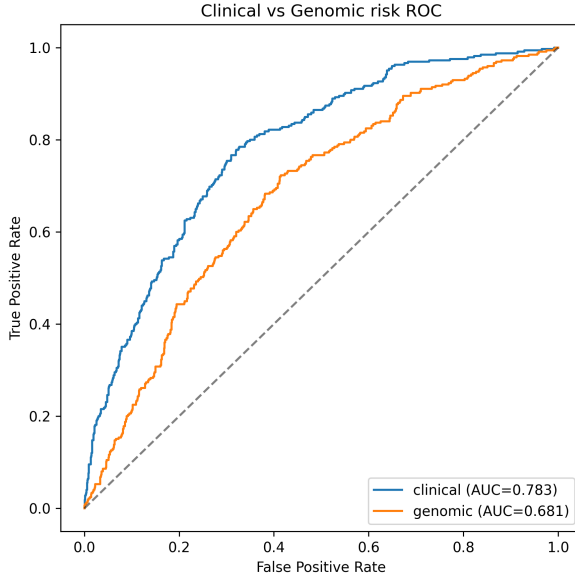


Figure 1: ROC curves for 5-year cancer-death prediction using cross-validated clinical and genomic random forest risk scores.

Figure 3 shows a scatterplot of clinical and genomic risk scores, with points colored by 5-year outcome. The two scores are positively related: patients with higher clinical risk usually also have higher genomic risk, forming a slanted cloud of points. Most 5-year deaths (coded as 1) appear in the upper-right, where both scores are high, while survivors are more common in the lower-left, where both scores are low. This pattern leads us to use copula analysis, so we can model the joint distribution of the two scores and focus on patients who are at high risk in both.

Since both clinical and genomic models provide prognostic information, and their risk scores are positively related, we now examine more closely how the two scores interact using copula models.

Copula-based Dependence Between Clinical and Genomic Risk Scores

In this part, we examine how the clinical and genomic risk scores change together across their full range, paying special attention to the extremes. We used pseudo-observations from the ranked scores to fit Gaussian, Clayton, and Gumbel copulas and calculated their tail dependence coefficients.

Table 2 summarizes the fitted parameters and tail dependence. The Gaussian copula, with a correlation of $\rho \approx 0.63$, shows no tail dependence ($\lambda_L = \lambda_U = 0$), meaning the dependence is symmetric. The Clayton copula, with $\theta \approx 1.52$, shows strong lower-tail dependence ($\lambda_L \approx 0.63$, $\lambda_U = 0$), so low values of both scores are more likely to occur together. The Gumbel copula, with $\theta \approx 1.76$, exhibits no lower-tail dependence but clear upper-tail dependence ($\lambda_U \approx 0.52$), indicating that very high clinical and genomic risks often co-occur.

To compare how well each copula fits, we used the Cramér–von Mises statistic with a parametric bootstrap (1000 replicates per copula). Table 3 shows the results. The Gaussian copula had the smallest difference between the observed and model-based copulas (statistic $\approx 2.4 \times 10^{-5}$) and a very high bootstrap p -value of 0.997, meaning the data fit the Gaussian copula well. The Clayton and Gumbel copulas exhibited larger differences (statistics around

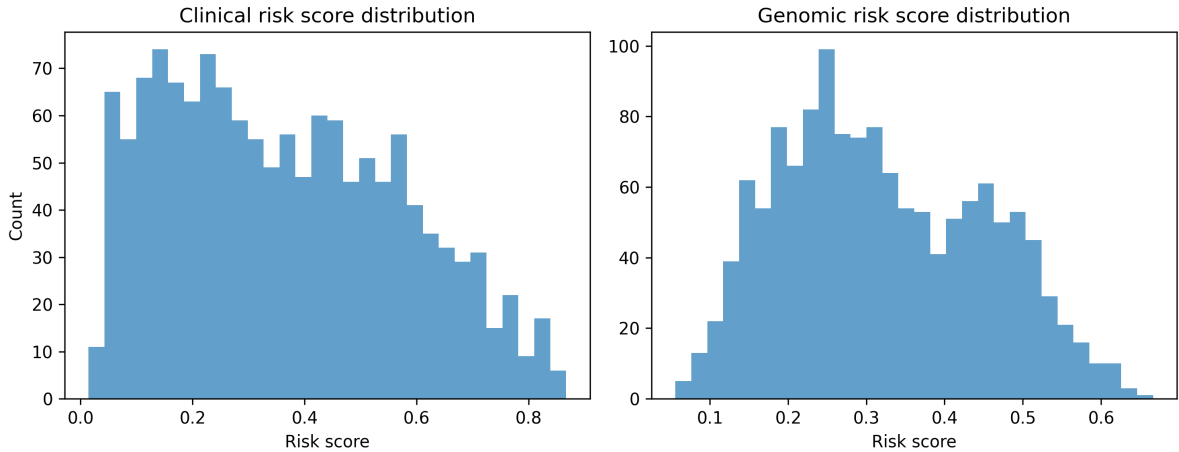


Figure 2: Distributions of cross-validated clinical (left) and genomic (right) risk scores for 5-year cancer death.

Table 2: Fitted copula parameters and tail dependence coefficients for the joint distribution of clinical and genomic risk scores.

Copula	Parameter	λ_L	λ_U
Gaussian	$\rho = 0.628$	0.000	0.000
Clayton	$\theta = 1.523$	0.634	0.000
Gumbel	$\theta = 1.761$	0.000	0.518

10^{-4}) and significantly lower p -values (0.176 and 0.413), indicating that they do not fit the data as well as the Gaussian model.

Table 3: Cramér–von Mises goodness-of-fit statistics and bootstrap p -values for fitted copulas.

Copula	Cramér–von Mises statistic	Bootstrap p -value
Gaussian	2.4×10^{-5}	0.997
Clayton	1.93×10^{-4}	0.176
Gumbel	9.81×10^{-5}	0.413

These numerical results match the graphical comparisons in Figure 4. The empirical copula heat map and the fitted Gaussian copula heat map look almost the same: both show a smooth gradient from low joint probabilities at $(u, v) = (0, 0)$ to high joint probabilities at $(1, 1)$, with no strong asymmetry. The contour plot in Figure 5 supports this, as the Gaussian copula contours fit the cloud of pseudo-observations well, following the main diagonal. Overall, these findings indicate that the clinical and genomic risk scores exhibit a moderate, mostly symmetric dependence, which the Gaussian copula represents well, with no indication of unusually frequent extreme risks occurring together.

Now that we have demonstrated that a Gaussian copula accurately describes the joint risk-score distribution, we ask whether this joint information is clinically relevant. In the next section, we categorize patients into high and low clinical and genomic scores and compare the differences in long-term survival among these four groups.

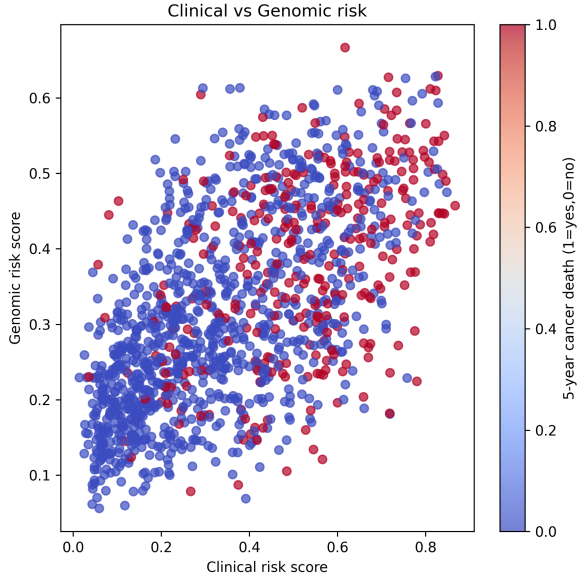


Figure 3: Joint scatterplot of cross-validated clinical and genomic risk scores, coloured by 5-year cancer-death outcome.

Joint Risk Strata and Survival

Here, we examine whether combining clinical and genomic risk scores yields meaningful differences in long-term survival. We used the median of each score to split patients into four groups: low-low (both scores at or below the median), high-clinical-only (clinical score above the median, genomic score at or below the median), high-genomic-only (genomic score above the median, clinical score at or below the median), and high-both (both scores above the median). For each group, we estimated Kaplan–Meier curves for overall survival using the original follow-up times and cancer-death indicators.

Figure 6 presents the survival curves. The low-low group has the best outcomes, showing the highest survival rates over time and a slower decline. Patients with high risk in only one score already have worse outcomes. Both the high-clinical-only and high-genomic-only groups have survival curves that are clearly lower than those of the low-low group, indicating that having either a high clinical or high genomic risk alone is associated with lower long-term survival.

The high-both group stands out. Its Kaplan–Meier curve falls the fastest and stays below those of the other groups throughout the follow-up, indicating the worst prognosis. Patients who are high risk in both models reach lower survival rates much sooner than those who are high risk in only one. This means that having both scores high leads to an even greater and clinically important drop in survival.

Overall, these results suggest that the clinical and genomic models each capture different parts of disease aggressiveness. The clinical score alone effectively separates patients, but when combined with a high genomic score, the joint information highlights a subgroup of patients with particularly poor long-term outcomes. In the next section, we summarise these findings and discuss what they could mean for risk stratification and future research.

In the next section, we summarise the main findings of this study and outline directions for future work.

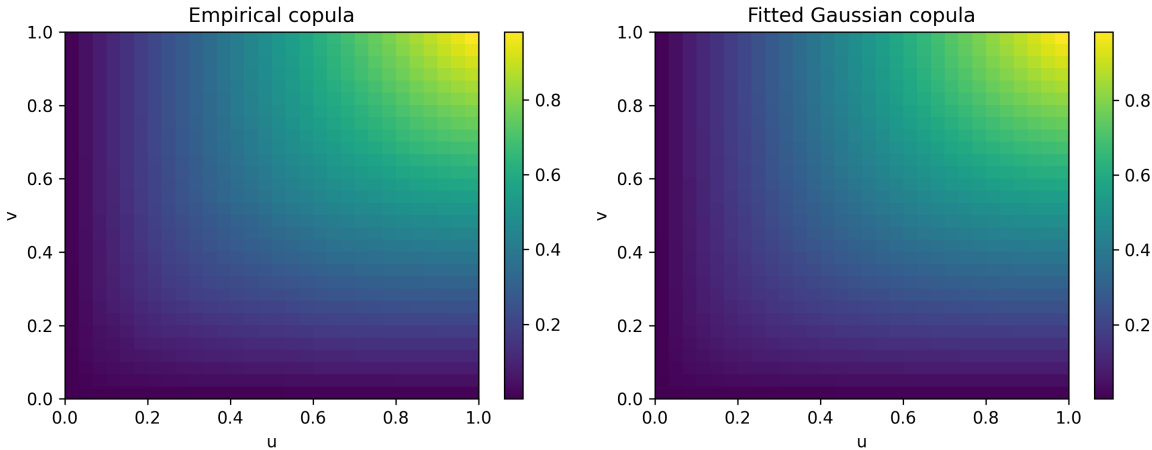


Figure 4: Empirical copula of the pseudo-observations (left) and fitted Gaussian copula (right) for the joint distribution of clinical and genomic risk scores.

Conclusion and Future Work

In this study, we aimed to determine whether combining clinical and genomic machine learning risk scores provides more prognostic information than using each model alone. Using the METABRIC breast cancer cohort, we built separate clinical and genomic models to predict 5-year cancer-specific mortality. The cross-validated AUCs indicated that the clinical model alone performed well (AUC approximately 0.78), while the genomic model also contributed moderate but meaningful predictive power (AUC approximately 0.68). This shows that both models offer complementary insights into disease aggressiveness.

Next, we examined the relationship between the clinical and genomic risk scores using copulas. We converted the scores to a common scale and fitted Gaussian, Clayton, and Gumbel copulas. The Gaussian copula fit the data best, with the smallest Cramér-von Mises discrepancy and the highest bootstrap p -value. This means the two scores are mostly symmetrically and positively related. The Gumbel copula also exhibited non-zero upper tail dependence (approximately 0.52), indicating that some patients are likely to be in the high-risk group for both scores simultaneously. In other words, if one model identifies a patient as very high risk, the other model is also more likely to do so.

Finally, we applied these findings on dependence to patient-level risk stratification. We grouped patients into four categories based on whether their clinical and genomic scores were above or below the median. This approach showed a clear and easy-to-understand separation of Kaplan-Meier curves. The low-low group had the best long-term survival, patients at high risk in only one area had intermediate outcomes, and the high-both group had the worst prognosis during follow-up. This result supports the main idea of the study: copula-based joint risk analysis can identify patients whose high clinical and genomic risk leads to especially poor survival.

This work has several limitations that point directly to future extensions. First, we focused on a single processed version of METABRIC and a relatively simple definition of the 5-year endpoint. In future work, the analysis could be repeated with alternative censoring choices, competing-risk formulations, or harmonised endpoints across multiple cohorts to assess robustness and external validity. Second, we restricted our machine learning models to regularised

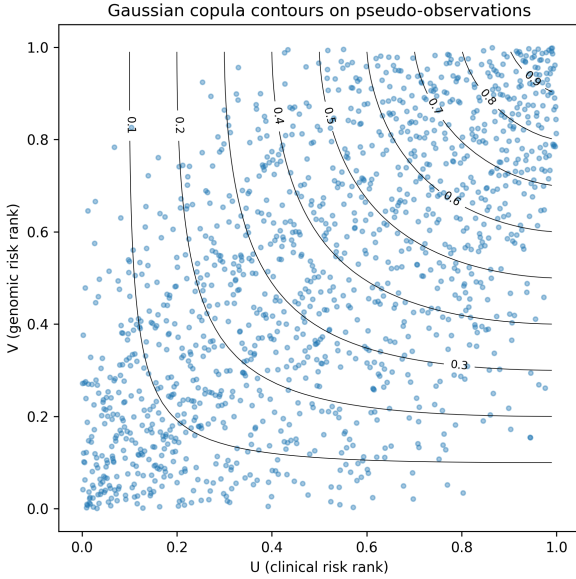


Figure 5: Gaussian copula contours overlaid on the pseudo-observations derived from the clinical and genomic risk scores.

logistic regression and tree-based ensembles. More flexible survival-aware models, such as gradient boosting for survival, random survival forests, or neural network-based survival models, could be explored, provided that out-of-sample risk scores are still available for copula estimation. Third, our copula analysis focused on just one clinical and one genomic score. In real-world settings, clinicians may want to incorporate other types of data, such as imaging scores or treatment-specific risk predictions. Expanding the framework to handle more data types using vine or factor copulas would enable multi-view analysis while maintaining the separation of modeling individual scores and their relationships. Another possible direction is to allow the copula parameters to change based on baseline patient characteristics, thereby varying the strength of the clinical-genomic link across different subtypes or treatment groups.

In this study, we only used standard copula families such as Gaussian, Clayton, and Gumbel. For datasets where the joint signal between views is significantly stronger than in METABRIC, more specialized copulas may be beneficial. Novel A1 and A2 Archimedean copulas [Aich et al., 2025, Aich, 2025] show very strong tail dependence and are only defined for Kendall’s τ above about 0.545, making them good options when clinical and genomic scores are almost perfectly matched at the extremes. Future research could explore A1 and A2 as alternative dependence models in cases where the link between risk scores is stronger than in this study, and compare their performance to that of the standard families used.

In summary, this study demonstrates that copula-based models for clinical and genomic risk scores are effective in a real-world population of breast cancer patients. The joint dependency structure helps find patients with especially poor long-term survival.

Data availability

The METABRIC cohort dataset was accessed via Kaggle using the link <https://www.kaggle.com/datasets/raghadalharbi/breast-cancer-gene-expression-profiles-metabric>.

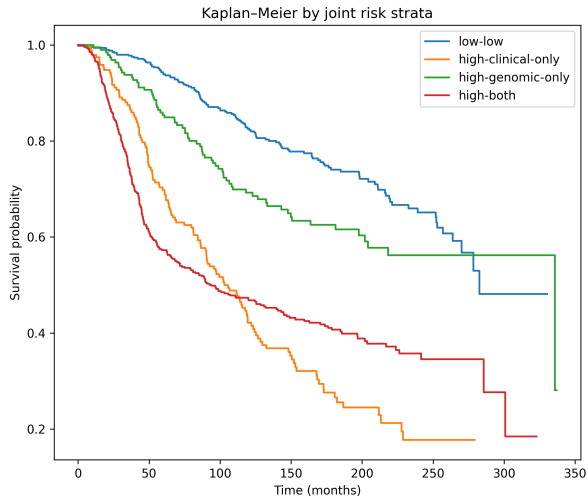


Figure 6: Kaplan–Meier curves for overall survival by joint risk group, defined using the medians of the clinical and genomic risk scores.

Code availability

All code to reproduce the analyses is available at

<https://github.com/agnivibes/copula-risk-fusion-genomics-ml>.

References

Agnideep Aich. Ignis: A robust neural network framework for constrained parameter estimation in archimedean copulas. *arXiv preprint arXiv:2505.22518*, 2025. doi: 10.48550/arXiv.2505.22518.

Agnideep Aich, A. B. Aich, and B. Wade. Two new generators of archimedean copulas with their properties. *Communications in Statistics—Theory and Methods*, 54(17):5566–5575, 2025. doi: 10.1080/03610926.2024.2440577.

Freddie Bray, Jacques Ferlay, Isabelle Soerjomataram, Rebecca L. Siegel, Lindsey A. Torre, and Ahmedin Jemal. Global cancer statistics 2018: GLOBOCAN estimates of incidence and mortality worldwide for 36 cancers in 185 countries. *CA: A Cancer Journal for Clinicians*, 68(6):394–424, 2018. doi: 10.3322/caac.21492.

Leo Breiman. Random forests. *Machine Learning*, 45(1):5–32, 2001. doi: 10.1023/A:1010933404324.

Tianqi Chen and Carlos Guestrin. Xgboost: a scalable tree boosting system. In *Proceedings of the 22nd ACM SIGKDD International Conference on Knowledge Discovery and Data Mining*, pages 785–794, 2016. doi: 10.1145/2939672.2939785.

David G. Clayton. A model for association in bivariate life tables and its application in epidemiological studies of familial tendency in chronic disease incidence. *Biometrika*, 65(1):141–151, 1978. doi: 10.2307/2335289.

D. R. Cox. The regression analysis of binary sequences. *Journal of the Royal Statistical Society: Series B*, 20(2):215–242, 1958. doi: 10.1111/j.2517-6161.1958.tb00292.x.

Christina Curtis, Sohrab P. Shah, Suet-Feung Chin, Gulisa Turashvili, Oscar M. Rueda, Mark J. Dunning, Doug Speed, Andy G. Lynch, Shamith Samarajiwa, Yinyin Yuan, Stefan Gräf, Gavin Ha, Gholamreza Haffari, Ali Bashashati, Roslin Russell, Steven McKinney, METABRIC Group, Anita Langerød, Andrew Green, Elena Provenzano, Gordon Wishart, Sarah Pinder, Peter Watson, Florian Markowetz, Leigh Murphy, Ian Ellis, Arnie Purushotham, Anne-Lise Børresen-Dale, James D. Brenton, Simon Tavaré, Carlos Caldas, and Samuel Aparicio. The genomic and transcriptomic architecture of 2,000 breast tumours reveals novel subgroups. *Nature*, 486(7403):346–352, 2012. doi: 10.1038/nature10983.

Jerome H. Friedman. Greedy function approximation: a gradient boosting machine. *Annals of Statistics*, 29(5):1189–1232, 2001. doi: 10.1214/aos/1013203451.

M. H. Galea, R. W. Blamey, C. E. Elston, and I. O. Ellis. The nottingham prognostic index in primary breast cancer. *Breast Cancer Research and Treatment*, 22(3):207–219, 1992. doi: 10.1007/BF01840834.

Alessandro Gasparini and Keith Humphreys. A natural history and copula-based joint model for regional and distant breast cancer metastasis. *Statistical Methods in Medical Research*, 31(12):2415–2430, 2022. doi: 10.1177/09622802221122410.

Christian Genest and Louis-Paul Rivest. Statistical inference procedures for bivariate archimedean copulas. *Journal of the American Statistical Association*, 88(423):1034–1043, 1993. doi: 10.1080/01621459.1993.10476372.

Christian Genest, Jean-François Quesey, and Bruno Rémillard. Asymptotic local efficiency of cramér-von mises tests for multivariate independence. *The Annals of Statistics*, 35(1): 166–191, 2007. doi: 10.1214/009053606000000984.

Christian Genest, Bruno Rémillard, and David Beaudoin. Goodness-of-fit tests for copulas: A review and a power study. *Insurance: Mathematics and Economics*, 44(2):199–213, 2008. doi: 10.1016/j.insmatheco.2007.10.005.

Emil J. Gumbel. Bivariate exponential distributions. *Journal of the American Statistical Association*, 55(292):698–707, 1960. doi: 10.1080/01621459.1960.10483368.

P. Hougaard. A class of multivariate failure time distributions. *Biometrika*, 73:671–678, 1986. doi: 10.2307/2336531.

Harry Joe. *Multivariate Models and Dependence Concepts*. Chapman and Hall/CRC, 1997. doi: 10.1201/9780367803896.

E. L. Kaplan and Paul Meier. Nonparametric estimation from incomplete observations. *Journal of the American Statistical Association*, 53(282):457–481, 1958. doi: 10.1080/01621459.1958.10501452.

Jong-Min Kim. Treatment effect estimation in survival analysis using copula-based deep learning models for causal inference. *Axioms*, 14(6):458, 2025. doi: 10.3390/axioms14060458.

Zhaoqi Liu, Xiang-Sun Zhang, and Shihua Zhang. Breast tumor subgroups reveal diverse clinical prognostic power. *Scientific Reports*, 4:4002, 2014. doi: 10.1038/srep04002.

Richard E. Neapolitan and Xia Jiang. Study of integrated heterogeneous data reveals prognostic power of gene expression for breast cancer survival. *PLOS ONE*, 10(2):e0117658, 2015. doi: 10.1371/journal.pone.0117658.

R. B. Nelsen. *An Introduction to Copulas*. Springer, New York, 2nd edition, 2006. doi: 10.1007/0-387-28678-0.

Soonmyung Paik, Steven Shak, Gong Tang, Charles Kim, Joseph Baker, Mark Cronin, et al. A multigene assay to predict recurrence of tamoxifen-treated, node-negative breast cancer. *New England Journal of Medicine*, 351(27):2817–2826, 2004. doi: 10.1056/NEJMoa041588.

Joel S. Parker, Maggie Mullins, Cheang Maggie C. U., Samuel Leung, et al. Supervised risk predictor of breast cancer based on intrinsic subtypes. *Journal of Clinical Oncology*, 27(8): 1160–1167, 2009. doi: 10.1200/JCO.2008.18.1370.

Bernard Pereira, Suet-Feung Chin, Oscar M. Rueda, Hans-Kristian Moen Volland, Elena Provenzano, Helen A. Bardwell, Michelle Pugh, Linda Jones, Roslin Russell, Stephen-John Sammut, Dana W. Y. Tsui, Bin Liu, Sarah-Jane Dawson, Jean Abraham, Helen Northen, John F. Peden, Abhik Mukherjee, Gulisa Turashvili, Andrew R. Green, Steve McKinney, Arusha Oloumi, Sohrab Shah, Nitzan Rosenfeld, Leigh Murphy, David R. Bentley, Ian O. Ellis, Arnie Purushotham, Sarah E. Pinder, Anne-Lise Børresen-Dale, Helena M. Earl, Paul D. Pharoah, Mark T. Ross, Samuel Aparicio, and Carlos Caldas. The somatic mutation profiles of 2,433 breast cancers refines their genomic and transcriptomic landscapes. *Nature Communications*, 7:11479, 2016. doi: 10.1038/ncomms11479.

Peter M. Ravdin, Laura A. Siminoff, Gary J. Davis, et al. Computer program to assist in making decisions about adjuvant therapy for women with early breast cancer. *Journal of Clinical Oncology*, 19(4):980–991, 2001. doi: 10.1200/JCO.2001.19.4.980.

Ozge Sahin and Harry Joe. Vine copula-based classifiers with applications. *Journal of Classification*, 42(2):335–363, 2024. doi: 10.1007/s00357-024-09494-y.

Gary A. Satten. Rank-based inference in the proportional hazards model for interval-censored data. *Biometrika*, 83(2):355–370, 1996. doi: 10.1093/biomet/83.2.355.

Jianhui Shih and Thomas A. Louis. Inferences on the association parameter in copula models for bivariate survival data. *Biometrics*, 51(4):1384–1399, 1995. doi: 10.2307/2533269.

Abe Sklar. Functions of distribution in n dimensions and their margins. *Publications de l'Institut de Statistique de l'Universite de Paris*, 8:229–231, 1959.

Nanang Susyanto, Chris A. J. Klaassen, Raymond N. J. Veldhuis, and Luuk J. Spreeuwers. Semiparametric score level fusion: Gaussian copula approach. In *Proceedings of the 36th WIC Symposium on Information Theory in the Benelux*, pages 26–33, Brussels, 2015.

Laura J. van 't Veer, Hongyue Dai, Marc J. van de Vijver, Yudong D. He, et al. Gene expression profiling predicts clinical outcome of breast cancer. *Nature*, 415(6871):530–536, 2002. doi: 10.1038/415530a.

Gordon C. Wishart, Elizabeth M. Azzato, David C. Greenberg, et al. Predict: a new UK prognostic model for early breast cancer that includes HER2. *British Journal of Cancer*, 103 (5):695–702, 2010. doi: 10.1186/bcr2464.

Qingyang Zhang and Xuan Shi. A mixture copula bayesian network model for multimodal genomic data. *bioRxiv*, page 110288, 2017. doi: 10.1101/110288.

Hui Zou and Trevor Hastie. Regularization and variable selection via the elastic net. *Journal of the Royal Statistical Society: Series B*, 67(2):301–320, 2005. doi: 10.1111/j.1467-9868.2005.00503.x.